Experimental evidence for fluvial bedrock incision by suspended and bedload sediment

Joel S. Scheingross[1*], Fanny Brun[1,2], Daniel Y. Lo[1], Khadijah Omerdin[1], and Michael P. Lamb[1]
[1]Division of Geological and Planetary Sciences, California Institute of Technology, Pasadena, California 91125, USA
[2]Geosciences Department, Ecole Normale Supérieure, 24 rue Lhomond, 75005 Paris, France

ABSTRACT

Fluvial bedrock incision sets the pace of landscape evolution and can be dominated by abrasion from impacting particles. Existing bedrock incision models diverge on the ability of sediment to erode within the suspension regime, leading to competing predictions of lowland river erosion rates, knickpoint formation and evolution, and the transient response of orogens to external forcing. We present controlled abrasion mill experiments designed to test fluvial incision models in the bedload and suspension regimes by varying sediment size while holding fixed hydraulics, sediment load, and substrate strength. Measurable erosion occurred within the suspension regime, and erosion rates agree with a mechanistic incision theory for erosion by mixed suspended and bedload sediment. Our experimental results indicate that suspension-regime erosion can dominate channel incision during large floods and in steep channels, with significant implications for the pace of landscape evolution.

INTRODUCTION

River incision into bedrock controls the flux of sediment to basins, links hillslopes to channels, and dictates the rate at which landscapes evolve (e.g., Whipple et al., 2013). Bedrock incision theory allows predictions of fluvial response to external perturbations, and the most commonly used models assume that erosion is proportional to stream power or bed shear stress (e.g., Howard and Kerby, 1983). Such models have been widely used in landscape evolution modeling (e.g., Tucker and Slingerland, 1994), as well as in studies examining feedbacks between climate, tectonics, and topography (e.g., Willett, 1999). However, stream-power models do not explicitly capture the physical processes of river erosion (i.e., the coupling of fluid flow, sediment transport, and channel erosion), limiting their predictive ability.

An alternative approach is to more directly account for processes eroding rock. The saltation-abrasion model (Sklar and Dietrich, 2004) predicts river-bed abrasion from single-sized sediment transported in bedload over a planar bed, and several of its basic tenets have been confirmed in laboratory and field settings (e.g., Sklar and Dietrich, 2001; Johnson and Whipple, 2010). This has led the model, and other similar models (e.g., Turowski et al., 2007), to be widely adopted in predicting reach-scale erosion (e.g., Cook et al., 2012), river-profile evolution (e.g., Crosby et al., 2007), and landscape evolution (e.g., Egholm et al., 2013). The saltation-abrasion model differs from the stream-power model in important and sometimes counterintuitive ways. For example, the saltation-abrasion model predicts decreased erosion rates for heightened bed shear stresses, leading to slower transient river network response to base-level change (Crosby et al., 2007; Gasparini et al., 2007), the preservation of relief in tectonically inactive mountain ranges over much longer time scales than with stream-power modeling (Egholm et al., 2013), and the formation of landforms that do not arise in stream-power modeling, such as permanent fluvial hanging valleys (Crosby et al., 2007) and static knickpoints that can grow infinitely in height (Sklar and Dietrich, 2008). In addition, in sand- and silt-bedded rivers and deltas where the majority of bed sediment is transported in suspension during floods, the saltation-abrasion model predicts zero erosion, counter to stream-power predictions and field observations of fluvial incision into consolidated sediment (Nittrouer et al., 2011; Shaw et al., 2013).

Differences between the saltation-abrasion and stream-power models arise, in part, because the saltation-abrasion model assumes an infinite hop length for particles transported within the suspension regime, such that particles are assumed not to impact the bed and erosion rates are predicted to be zero (Sklar and Dietrich, 2004, 2006). The transition from the bedload regime to the suspension regime is often defined as the point in which bed shear velocity, u_* (a fluid turbulence proxy), surpasses particle terminal settling velocity, w_s (Bagnold, 1966; McLean, 1992), such that turbulence strongly influences particle trajectories. In the suspension regime, some particles are advected high into the water column by turbulence (i.e., the suspended load); however, the largest concentration of particles is still near the bed (Rouse, 1937) where particles impact the bed via rolling, sliding, and saltation (i.e., bedload), and there is active exchange of particles between the bedload layer and suspended load above (e.g., McLean, 1992; Garcia and Parker, 1993). To account for erosion due to particle-bed impacts within the suspension regime, the saltation-abrasion model was recast (by Lamb et al., 2008) in terms of near-bed sediment concentration rather than particle hop lengths (herein referred to as the total-load model). The saltation-abrasion and total-load models produce similar results for erosion within the bedload regime, but within the suspension regime the total-load model predicts nonzero erosion rates that increase with increasing fluid bed stress, leading to contrasting predictions for landscape evolution, especially during large floods and in steep channels where bed sediment is suspended.

Laboratory experiments offer a means to test the validity of existing bedrock-erosion theories under controlled conditions that are otherwise difficult to achieve in natural rivers. Previous experimental work suggests that channel-bed erosion in the suspension regime is possible (Sklar and Dietrich, 2001; Cornell, 2007; Chatanantavet et al., 2010), but experiments have not been conducted that allow full testing of existing models within the suspension regime. Herein we present results from controlled abrasion mill experiments and find significant rates of erosion within the suspension regime, in agreement with the total-load erosion model; these results have important implications for landscape evolution.

EXPERIMENTAL SETUP

In natural river channels, erosion rates are likely influenced by multiple sediment sizes in transport, complex bed topography, and jointed rock that may promote plucking (e.g., Hancock et al., 1998). Our goal is not to reproduce this complexity, but rather to test the competing predictions of the saltation-abrasion and total-load erosion models under the simplest possible scenarios and in accordance with inherent assumptions in the models, including single-sized sediment, and a planar river bed of massive, unjointed rock. Testing existing models under these simplified conditions is important because such baseline tests have yet to be performed, and the existing theories are widely applied to natural landscapes and used in landscape evolution simulations despite these assumptions (e.g., Cook et al., 2012; Egholm et al., 2013).

To explore bedrock erosion rates over a wide range of transport conditions, we conducted experiments in abrasion mills (Fig. 1) identical to those used by Sklar and Dietrich (2001) in their study of erosion rates in the bedload regime. In abrasion mills, suspension of sedi-

*E-mail: jscheingross@caltech.edu.

 Data Repository item 2014185 | doi:10.1130/G35432.1
© 2014 Geological Society of America. For permission to copy, contact Copyright Permissions, GSA, or editing@geosociety.org.

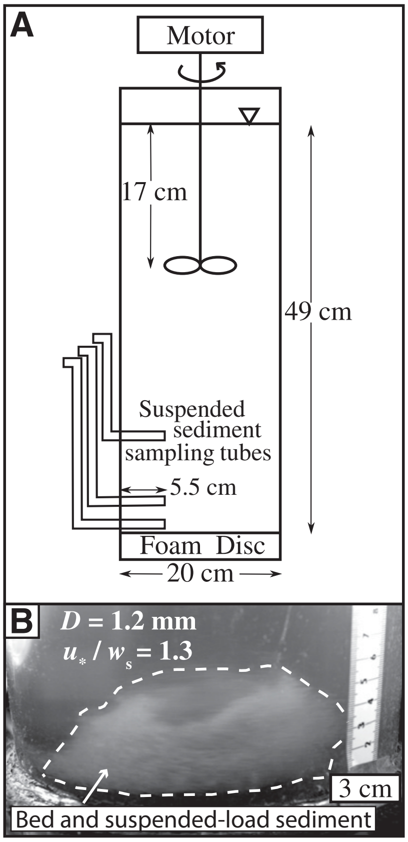

Figure 1. A: Schematic diagram of abrasion mill and sediment concentration measurement system (modified from Sklar and Dietrich, 2001). B: Contrast-enhanced, side-view photograph of suspension-regime transport within an abrasion mill. *D*—grain diameter; u_*—bed shear velocity; w_s—particle terminal settling velocity.

ment can be achieved by increasing the flow speed (i.e., increasing u_*), decreasing the sediment size (i.e., decreasing w_s), or both. Increasing flow speed to suspend gravel in the abrasion mills is problematic, however, because higher flow speeds require larger diameter mills to eliminate covarying changes in secondary flow circulation. Thus, we chose to conduct experiments by varying sediment diameter ($0.46 < D < 44$ mm; Table DR1 in the GSA Data Repository[1]) to achieve flow conditions spanning both the suspension and bedload regimes ($0.15 < u_*/w_s < 2.9$), while holding propeller speed (1000 rpm, $u_* \approx 0.15$ m/s; Sklar and Dietrich, 2004) and total sediment load (70 g) constant to match previous experiments (Sklar and Dietrich, 2001). Note that under the imposed conditions of constant sediment load and flow speed, finer sediment will necessarily produce smaller erosion rates, regardless of whether transport is in the suspension regime, because of smaller particle mass and fall velocity. Erosion rates should also approach zero with decreasing grain size as impacts become viscously damped for particle Stokes numbers (St, a nondimensional number that weights the kinetic energy of particle impacts to the fluid viscosity) below ~10–100 (Joseph et al., 2001).

To achieve measurable erosion rates, we used low-tensile-strength (σ_T = 0.32 MPa) polyurethane foam as a highly erodible bedrock simulant rather than natural rock. Tests show that foam follows the same erosion-rate scaling relationship with tensile strength as observed by Sklar and Dietrich (2001) for rock and concrete (see the Data Repository, and Fig. DR1 therein), allowing our results to be properly scaled to natural rock.

For each experiment, we secured a 38-mm-thick foam disc to the base of the abrasion mill, loaded the mill with siliciclastic, well-sorted, subangular to subrounded sediment, and filled the mill to a depth of 49 cm with water. A propeller induced flow and sediment transport, and experiments were run long enough for measurable wear of the foam disc by either volume loss (using a submillimeter-precision laser scanner) or mass loss (using a 0.1 g precise scale), depending on total volume eroded. For grain diameters $D \le 2.4$ mm we collected flow samples at 3 elevations above the bed (1, 3, and 10 cm) to quantify the suspended sediment concentration profile (Fig. 1; see the Data Repository).

SEDIMENT TRANSPORT

Using a transparent mill, we observed that grains with $D \ge 7$ mm ($u_*/w_s \le 0.44$) were transported exclusively in bedload, moving via rolling, sliding, and saltating along the bed, grains with $D \le 1.2$ mm ($u_*/w_s \ge 1.3$) moved in both bedload and suspended load, and grains with *D* ~2.0–2.4 mm ($0.61 \le u_*/w_s \le 1.0$) were intermediate between exclusive bedload and intermittent suspension (Fig. DR2; Movies DR1–DR4). In the radial direction, sediment concentrated in an annulus around the center of the mill due to secondary circulation (Sklar and Dietrich, 2001, 2004); however, secondary circulation was typically <~10% of the mean azimuthal flow velocity and did not appear to strongly influence erosion rates (see the Data Repository).

Measurements of sediment concentration, *c*, for $D < 2$ mm had vertical profiles (Fig. 2) comparable to that predicted by classic theory (Rouse, 1937),

$$c = c_b \left[\frac{\left(\frac{1}{z}\right) - \left(\frac{1}{H}\right)}{\left(\frac{1}{H_b}\right) - \left(\frac{1}{H}\right)} \right]^{\frac{w_s}{\beta \kappa u_*}}, \tag{1}$$

where *z* is height above the bed, *H* is flow depth, c_b and H_b are near-bed sediment concentration and bedload layer thickness (calculated following Lamb et al., 2008), β is a dimensionless constant weighting the diffusivities of sediment relative to fluid momentum, and κ = 0.41 is von Karman's constant. Despite the different flow hydraulics in abrasion mills versus the unidirectional, steady, turbulent boundary layer assumed in the derivation of Equation 1, the Rouse model shows reasonable agreement with our measurements for β = 2 (Fig. 2), a value similar to that found in unidirectional flows (e.g., β = 0.5–3; Graf and Cellino, 2002).

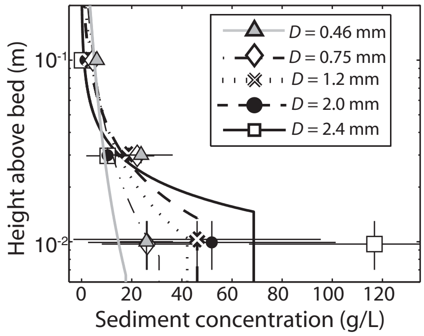

Figure 2. Rouse sediment concentration profiles (dashed and solid lines) for different grain diameters (*D*) with β = 2 (β is a dimensionless constant weighting the diffusivities of sediment relative to fluid momentum), for total sediment load of 70 g. Symbols correspond to mean of sediment concentration measurements (n = 3); x- and y-error bars represent geometric standard deviation of measurements and radius of sampling tubing (3 mm), respectively.

BEDROCK EROSION

Measurable erosion of synthetic bedrock occurred in all experiments, including those within the suspension regime. Under fixed total sediment load, erosion rates decreased with decreasing grain size from ~10^2 cm^3/h for the largest grains that were transported in the bedload regime (D = 40 mm, u_*/w_s = 0.15) to ~10^{-2} cm^3/h for the smallest grains that were transported in the suspension regime (D = 0.46 mm, u_*/w_s = 2.9) (Fig. 3A; Table DR1). The observed erosion rate versus grain-size relationship for the bedload regime matches that observed by Sklar and Dietrich (2001) for grains eroding limestone, except that we observed higher erosion rates due to the use of a lower tensile strength substrate. To directly compare our results to those of Sklar and Dietrich (2001) we scaled volumetric foam erosion rates ($E_{v\text{-}f}$) to equivalent values for erosion of limestone ($E_{v\text{-}ls}$) using the tensile-strength scaling relationship proposed by Sklar and Dietrich (2001) and confirmed here (Fig. DR1B):

$$E_{v\text{-}ls} = E_{v\text{-}f} \left(\frac{\sigma_{T\text{-}ls}}{\sigma_{T\text{-}f}} \right)^{-2}, \tag{2}$$

where $\sigma_{T\text{-}f}$ and $\sigma_{T\text{-}ls}$ are the tensile strengths of foam (0.32 MPa) and limestone (9.8 MPa),

[1]GSA Data Repository item 2014185, supplementary text, figures, movies, and tables, is available online at www.geosociety.org/pubs/ft2014.htm, or on request from editing@geosociety.org or Documents Secretary, GSA, P.O. Box 9140, Boulder, CO 80301, USA.

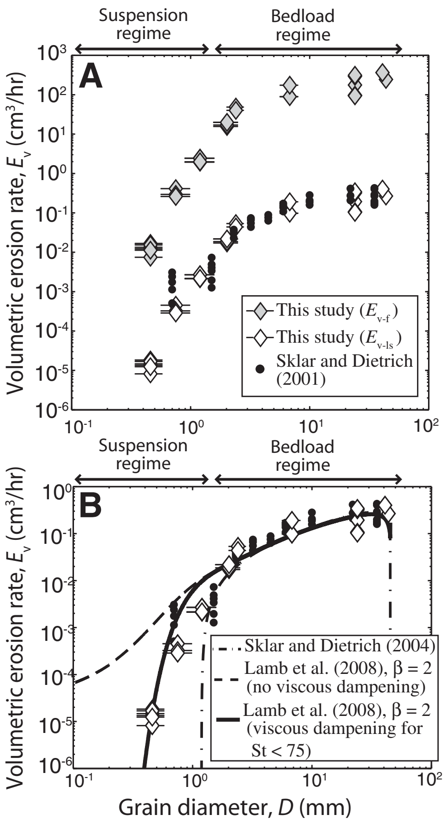

Figure 3. A: Volumetric erosion rate (E_v) versus grain diameter (D) in this study and from previous experiments eroding limestone. We show both measured foam erosion rates ($E_{v\text{-}f}$) and limestone-equivalent rates ($E_{v\text{-}ls}$; see Equation 2). Error bars correspond to limits of unimodal grain size distributions as reported in Table DR1 (see footnote 1). B: As in A; lines show theoretical predictions of saltation-abrasion model (Sklar and Dietrich, 2004), and total-load model (Lamb et al., 2008) with and without viscous dampening. Cover term was neglected due to low sediment loading, and nondimensional constant k_v was set to 3×10^5 to account for the fact that particle tensile strength was greater than substrate tensile strength (for details, see Sklar and Dietrich, 2004). St—Stokes number.

respectively. The scaled foam data collapse to nearly the same values found by Sklar and Dietrich (2001), and extend the combined data set to smaller sediment sizes with higher u_*/w_s (Fig. 3A).

The saltation-abrasion model (Sklar and Dietrich, 2004) predicts zero erosion for $D < \sim 2$ mm due to the onset of suspension; this does not match our data (Fig. 3B). The total-load model (Lamb et al., 2008), however, overpredicts erosion rates within the suspension regime when viscous dampening of impacts is neglected. The best model fit to the data is the total-load abrasion model where impacts are viscously damped for St < 75; this value is within the range of partial dampening found in particle-wall collision studies (e.g., Joseph et al., 2001).

DISCUSSION AND IMPLICATIONS

Our experimental results provide direct evidence for fluvial incision in the suspension regime, show that viscous dampening reduces erosion rates for low-energy impacts, and support the use of the total-load model for predicting erosion in both the bedload and suspension regimes. Our observations show that suspension-regime erosion occurs because particles are transported both in a bedload layer with high sediment concentrations near the bed, and in a more dilute suspended-load layer above (e.g., Fig. 2; Fig. DR2), with active interchange of particles between the two layers and active particle-bed impacts. Erosion rates in our experiments decreased across the bedload to suspension regime primarily because we decreased grain size while holding sediment load and flow speed constant, and, under these conditions, smaller particles have lower kinetic energy upon impact, regardless of the transport mode. The total-load model predicts that suspension-regime erosion rates would be of a magnitude similar to that of bed-load-regime rates if experiments were instead conducted by varying u_* while holding grain size constant (Fig. 4), and would outpace bedload regime rates by several orders of magnitude if sediment load increases with u_* (see the Data Repository; Fig. DR3). Although more difficult experimentally, these

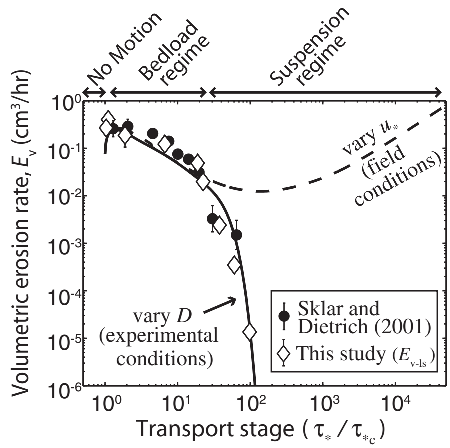

Figure 4. Volumetric erosion rate, E_v, versus transport stage, τ_*/τ_{*c}, for abrasion mill experiments, where τ_* and τ_{*c} are the Shields stress and critical Shields stress, respectively. Lines show theoretical predictions of total-load model (Lamb et al., 2008) for transport stage varied by changing grain size (diameter, D, solid line), as was done in the abrasion mill experiments, and by changing shear velocity (u_*) with constant flow depth (dashed line). Symbols show mean and 1σ standard deviation of erosion rates for abrasion mill experiments, with foam erosion rates converted to limestone-equivalent rates ($E_{v\text{-}ls}$) using Equation 2 (see text). Models include viscous dampening of impacts for particle Stokes number < 75, β = 2, $k_v = 3 \times 10^5$ (nondimensional constant), and neglect cover.

alternate scenarios are likely in natural rivers during floods, suggesting that erosion by sediment in the suspension regime may be more important in natural rivers than demonstrated in our experiments.

In natural rivers, the relative efficiency of erosion within the suspension regime depends strongly on the ability of a flood to suspend bed sediment. Bankfull floods in gravel-bed rivers rarely suspend bed material (Parker et al., 2007), such that, for typical mass flux ratios of bed to suspended load, erosion from gravel and cobbles moving exclusively in bedload likely outpace suspension-regime erosion from sand and silt, which have smaller impact velocities, and impacts may be viscously damped.

Suspension-regime erosion will dominate fluvial abrasion when bed sediment is suspended, however, which regularly occurs in sand-bedded rivers, in coarse-grained rivers during large floods, and in steep channels and knickzones. For example, the total-load model successfully predicts erosion of consolidated mud in the Wax Lake Delta (Louisiana), where the majority of grain sizes present on the bed are transported in the suspension regime during bankfull flows (Shaw et al., 2013). These conditions are common in other lowland distributary rivers (e.g., Nittrouer et al., 2011), where the dominance of suspension-regime transport would cause the saltation-abrasion model to erroneously predict zero erosion. Suspension of bed material can also occur during large-magnitude storms in coarse-bedded mountain rivers. For example, typhoon-induced floods in the Da'an River, Taiwan, resulted in ~20 m of vertical incision over a 4 yr period (Cook et al., 2012). We calculate that grains as large as 1 m in diameter were within the suspension regime in the narrowest portion of the gorge, where erosion was rapid (see the Data Repository); this is far larger than the median grain diameter of the bed material (15 cm; Cook et al., 2012), suggesting that the bulk of erosion occurred within the suspension regime.

In landscape evolution modeling, suspension-regime erosion causes erosion rates to increase on steep channel slopes, similar to stream-power models (Fig. DR3), and may prevent formation of oversteepened, nonerod-ing reaches that develop in simulations that use the saltation-abrasion model (e.g., Wobus et al., 2006; Crosby et al., 2007; Sklar and Dietrich, 2008). Suspension-regime erosion also allows steep river reaches to propagate more rapidly through a landscape, resulting in faster transmission of changes in base level than observed with saltation-abrasion models (Crosby et al., 2007; Gasparini et al., 2007), and this in turn may influence the predictions of morphology and lifespan of mountain ranges. For example, recent predictions using the saltation-abrasion model attribute the long-term preservation of relief in tectonically inactive mountain ranges to landslide-modulated sediment supply to river networks (Egholm et al., 2013). However, including suspension-regime erosion in modeling should yield higher erosion rates, which will more rapidly reduce relief both on steep slopes and under high rates of sediment supply if bed sediment is suspended (e.g., Fig. DR3).

ACKNOWLEDGMENTS

We thank Leonard Sklar for enlightening discussions and donation of an abrasion mill, and Chris Borstad for conversations on fracture mechanics. Brandon McElroy kindly measured our fine sediment sizes, and Brian Fuller built the abrasion mills. Discussion with Roman DiBiase, reviews from Phairot Chatanatavet, Nicole Gasparini, Leslie Hasbargen, Leonard Sklar, and an anonymous reviewer, and editorial comments from James Spotila greatly improved this manuscript. Support came from a National Science Foundation (NSF) Graduate Research Fellowship to Scheingross, NSF grant EAR-1147381 grant to Lamb, and a California Institute of Technology Summer Undergraduate Research Fellowship to Lo.

REFERENCES CITED

Bagnold, R.A., 1966, An approach to the sediment transport problem for general physics: U.S. Geological Survey Professional Paper 422-I, 37 p.

Chatanantavet, P., Whipple, K.X., and Adams, M.A., 2010, Experimental study of bedrock incision processes by both suspended load and bedload abrasions: American Geophysical Union Fall Meeting, abs. EP22A–04.

Cook, K.L., Turowski, J.M., and Hovius, N., 2012, A demonstration of the importance of bedload transport for fluvial bedrock erosion and knickpoint propagation: Earth Surface Processes and Landforms, v. 38, p. 683–695, doi:10.1002/esp.3313.

Cornell, K.M., 2007, Suspended sediment erosion in laboratory flume experiments [M.S. thesis]: Cambridge, Massachusetts Institute of Technology, 50 p.

Crosby, B.T., Whipple, K.X., Gasparini, N.M., and Wobus, C.W., 2007, Formation of fluvial hanging valleys: Theory and simulation: Journal of Geophysical Research, v. 112, no. F3, doi:10.1029/2006jf000566.

Egholm, D., Knudsen, M., and Sandiford, M., 2013, Lifespan of mountain ranges scaled by feedbacks between landsliding and erosion by rivers: Nature, v. 498, p. 475–478, doi:10.1038/nature12218.

Garcia, M., and Parker, G., 1993, Experiments on the entrainment of sediment into suspension by a dense bottom current: Journal of Geophysical Research, v. 98, p. 4793–4807, doi:10.1029/92JC02404.

Gasparini, N.M., Whipple, K.X., and Bras, R.L., 2007, Predictions of steady state and transient landscape morphology using sediment-flux-dependent river incision models: Journal of Geophysical Research, v. 112, no. F3, doi:10.1029/2006JF000567.

Graf, W.H., and Cellino, M., 2002, Suspension flows in open channels; experimental study: Journal of Hydraulic Research, v. 40, p. 435–447, doi:10.1080/00221680209499886.

Hancock, G.S., Anderson, R.S., and Whipple, K.X, 1998, Beyond power: Bedrock river incision process and form, *in* Tinkler, K., and Wohl, E.E., eds., Rivers over rock: Fluvial processes in bedrock channels: American Geophysical Union Geophysical Monograph 107, p. 35–60, doi:10.1029/GM107p0035.

Howard, A.D., and Kerby, G., 1983, Channel changes in badlands: Geological Society of America Bulletin, v. 94, p. 739–752, doi:10.1130/0016-7606(1983)94<739:CCIB>2.0.CO;2.

Johnson, J.P.L., and Whipple, K.X, 2010, Evaluating the controls of shear stress, sediment supply, alluvial cover, and channel morphology on experimental bedrock incision rate: Journal of Geophysical Research, v. 115, doi:10.1029/2009JF001335.

Joseph, G.G., Zenit, R., Hunt, M.L., and Rosenwinkel, A.M., 2001, Particle-wall collisions in a viscous fluid: Journal of Fluid Mechanics, v. 433, p. 329–346, doi:10.1017/S0022112001003470.

Lamb, M.P., Dietrich, W.E., and Sklar, L.S., 2008, A model for fluvial bedrock incision by impacting suspended and bed load sediment: Journal of Geophysical Research, v. 113, doi:10.1029/2007JF000915.

McLean, S.R., 1992, On the calculation of suspended-load for noncohesive sediments: Journal of Geophysical Research, v. 97, p. 5759–5770, doi:10.1029/91JC02933.

Nittrouer, J.A., Mohrig, D., Allison, M.A., and Peyret, A.P.B., 2011, The lowermost Mississippi River: A mixed bedrock-alluvial channel: Sedimentology, v. 58, p. 1914–1934, doi:10.1111/j.1365-3091.2011.01245.x.

Parker, G., Wilcock, P.R., Paola, C., Dietrich, W.E., and Pitlick, J., 2007, Physical basis for quasi-universal relations describing bankfull hydraulic geometry of single-thread gravel bed rivers: Journal of Geophysical Research, v. 112, doi:10.1029/2006JF000549.

Rouse, H.R., 1937, Modern conceptions of the mechanics of turbulence: American Society of Civil Engineers Transactions, v. 102, p. 463–543.

Shaw, J.B., Mohrig, D., and Whitman, S.K., 2013, The morphology and evolution of channels on the Wax Lake Delta, Louisiana, USA: Journal of Geophysical Research, v. 118, p. 1562–1584, doi:10.1002/jgrf.20123.

Sklar, L.S., and Dietrich, W.E., 2001, Sediment and rock strength controls on river incision into bedrock: Geology, v. 29, p. 1087–1090, doi:10.1130/0091-7613(2001)029<1087:SARSCO>2.0.CO;2.

Sklar, L.S., and Dietrich, W.E., 2004, A mechanistic model for river incision into bedrock by saltating bed load: Water Resources Research, v. 40, doi:10.1029/2003WR002496.

Sklar, L.S., and Dietrich, W.E., 2006, The role of sediment in controlling steady-state bedrock channel slope: Implications of the saltation-abrasion incision model: Geomorphology, v. 82, p. 58–83, doi:10.1016/j.geomorph.2005.08.019.

Sklar, L.S., and Dietrich, W.E., 2008, Implications of the saltation-abrasion bedrock incision model for steady-state river longitudinal profile relief and concavity: Earth Surface Processes and Landforms, v. 33, p. 1129–1151, doi:10.1002/esp.1689.

Tucker, G.E., and Slingerland, R.L., 1994, Erosional dynamics, flexural isostasy, and long-lived escarpments: A numerical modeling study: Journal of Geophysical Research, v. 99, p. 12229–12243, doi:10.1029/94JB00320.

Turowski, J.M., Lague, D., and Hovius, N., 2007, Cover effect in bedrock abrasion: A new derivation and its implications for the modeling of bedrock channel morphology: Journal of Geophysical Research, v. 112, doi:10.1029/2006JF000697.

Whipple, K.X., DiBiase, R.A., and Crosby, B.T., 2013, Bedrock rivers, *in* Shroder, J., Jr., and Wohl, E., eds., Fluvial geomorphology: Treatise on Geomorphology Volume 9: San Diego, California, Academic Press, doi:10.1016/B978-0-12-374739-6.00254-2.

Willett, S.D., 1999, Orogeny and orography: The effects of erosion on the structure of mountain belts: Journal of Geophysical Research, v. 104, p. 28957–28981, doi:10.1029/1999JB900248.

Wobus, C.W., Crosby, B.T., and Whipple, K.X, 2006, Hanging valleys in fluvial systems: Controls on occurrence and implications for landscape evolution: Journal of Geophysical Research, v. 111, doi:10.1029/2005JF000406.

Manuscript received 2 January 2014
Revised manuscript received 18 March 2014
Manuscript accepted 21 March 2014

Printed in USA

GSA DATA REPOSITORY 2014185

Experimental evidence for fluvial bedrock incision by suspended and bedload sediment

Joel S. Scheingross [1*], Fanny Brun[1,2], Daniel Y. Lo[1], Khadijah Omerdin[1], and Michael P. Lamb[1]

1. SCALING FOAM-TO-ROCK EROSION

The erosion rate of natural rock and concrete has been show to depend primarily on the substrate tensile strength, σ_T (Sklar and Dietrich, 2001). To test this scaling relationship for polyurethane foam, we designed a set of abrasion mill experiments eroding foam of different tensile strength (0.3< σ_T < 17 MPa, Table DR2) and density (0.06 to 0.96 g/cm^3) while holding all other variables constant, including sediment load (150 g) and grain size (D = 6 mm). These experiments are identical to erosion-rate versus tensile-strength experiments presented in Sklar and Dietrich (2001), except here we use a foam substrate rather than rock or concrete. Results show foam erosion rates by mass loss, E_m, varied inversely with tensile strength from ~10^1 to 10^{-2} g/hr, and were slightly lower than E_m measurements from Sklar and Dietrich (2001) for material of similar tensile strength (Fig. DR1A). Accounting for the low density of foam compared to rock results in a reasonable match between foam and rock erosion, where volumetric erosion rates, E_v, scale with σ_T^{-2} (Fig. DR1B). This agreement suggests that foam acts as a suitable rock analog.

Note that Sklar and Dietrich (2004) further proposed that erosion rate depends on material Young's Modulus, Y, and a (material specific) non-dimension constant, k_v. Unlike natural rock which has little variation in Y and k_v, the Young's Modulus of foam used in this study varied from 3.9 to 330 MPa. This implies that to achieve the observed relationship between foam tensile strength and erosion rate, either k_v must vary in proportion to Y (which goes against the theoretical expectation of constant k_v (Engle, 1978)), or that Young's Modulus may have little influence on erosion rate, as has recently been suggested (Beyeler et al., 2009). In either case, the agreement in erosion-rate versus tensile-strength relationship for foam, natural rock, and concrete allows results obtained between the three substrates to be directly compared.

2. SEDIMENT CONCENTRATION MEASUREMENTS

We sampled suspended and bedload sediment within abrasion mills using 6.4 mm diameter siphons inserted through the abrasion mill walls, a sampling velocity (~0.65 $\pm$ 0.1 m/s) similar to the mean flow velocity (Winterstein and Stefan, 1983), and sample volumes that did not exceed 1.75 L (~12% of the abrasion mill water volume). Sediment concentration was measured by weighing and drying the samples, and weighing the sediment.

3. SECONDARY CIRCULATION

We used high speed video (240 frames per second) looking up through the bottom of a clear abrasion mill with foam removed to track particle motion and quantify secondary flow circulation. We manually tracked individual particle trajectories for distances of 1 – 4 full rotations about the mill, and averaged trajectories over 7 frames to calculate the ratio of azimuthal to radial distance traveled. For five grains of 6.8 mm diameter, we found median values of azimuthal to radial distance traveled ranged from ~7 – 17. Particle trajectories for grains smaller than 6 mm could not be measured due to high particle velocities and small particle size which exceeded the speed and resolution of our high speed camera.

Sklar and Dietrich (2001; 2004) attributed suspension-regime erosion in abrasion mill experiments to secondary circulation, which they argued induced bedload transport in a way not representative of natural rivers. However, our observations are consistent with previous workers who showed that high concentrations of particles and active particle-bed interactions are expected near the bed (i.e., in a bedload layer) even within the suspension regime (e.g., Rouse, 1937; McLean, 1992). Furthermore, although secondary circulation is an important component of flow in the abrasion mills, several observations suggest it did not dominate particle trajectories or strongly influence bedrock erosion rates. First, secondary circulation in natural rivers with flow around bends as well as in straight channels is of similar magnitude (~10% of the mean azimuthal flow velocity (Dietrich and Smith, 1983; Nikora and Roy, 2012)) to our abrasion mill observations (Fig. DR2; Movies DR1–4). Second, the agreement between sediment-concentration measurements and Rouse-profile predictions (Fig. 2) suggest the abrasion mills reasonably replicate natural river fluid flow and sediment transport. Third, we observed fluting and grooves on the eroded foam surfaces parallel to the azimuthal flow direction, suggesting radial sediment transport due to secondary circulation did not exert a detectable influence on erosion.

4. ROLE OF SLOPE, FLOW DEPTH, SEDIMENT SIZE, AND SEDIMENT LOAD

Suspension of sediment during fluvial transport can be achieved either by decreasing particle size (i.e., lowering settling velocity, w_s), or increasing fluid shear stress (i.e., increasing shear velocity, u_*). In the experiments presented here, we decreased grain size while holding shear velocity and sediment load constant to achieve suspension. While tractable experimentally, this is not an ideal representation of natural bedrock rivers where the transition from bedload to suspension regime transport occurs primarily due to increases in shear velocity associated with flood events, which additionally tend to increase sediment supply (e.g., Leopold et al., 1964). Here we explore how changes in grain size, shear velocity, and sediment supply influence erosion rates in both the bedload and suspension regimes.

We ran the total-load and saltation-abrasion models under variable transport stage, τ_*/τ_{*c}, where τ_* is the non-dimensional Shields stress defined as

$$\tau_* = \frac{\tau}{\left(\rho_s - \rho_f\right) g D} \quad , \qquad \text{(DR1)}$$

τ is bed shear stress, g is acceleration due to gravity, ρ_s = 2650 kg/m^3 and ρ_f = 1000 kg/m^3 are the sediment and fluid densities, respectively, and τ_{*c} = 0.03 is the critical Shields stress for sediment motion. We assumed steady, uniform flow such that

$$\tau = \rho_f u_*^2 = \rho_f g h S \quad , \qquad \text{(DR2)}$$

where h and S are the channel flow depth and slope, respectively. Under these assumptions, increases in τ_*/τ_{*c} arise from increasing h or S, or decreasing D. The total-load model is dependent upon h and S individually, whereas the saltation-abrasion model is dependent upon shear velocity (i.e., the product hS). We varied transport stage to cover conditions from incipient motion to well within the suspension regime ($10^0 < \tau_*/\tau_{*c} < 10^4$). Values of τ_*/τ_{*c} do not correspond to identical values of u_*/w_s across different model runs; however, the transition from bedload to suspension regime transport generally occurs when τ_*/τ_{*c} exceeds ~20-40. We ran two separate scenarios, first for a constant sediment load, q_s, and second, letting $q_s = 0.5q_{sc}$, where $q_{sc} = 5.7(RgD^3)^{1/2}(\tau_* - \tau_{*c})^{3/2}$ is the sediment transport capacity calculated using the empirical fit of Fernandez Lueque and van Beek (1976), and $R = (\rho_s - \rho_f)/\rho_f$ is the submerged specific density of sediment. For all cases we used base conditions representative of the South Fork Eel River, California, USA (D = 60 mm, h = 0.95 m, S = 0.0053, $q_s = 8.9 \times 10^{-4}$ m^2/s), which has been used as a reference site for the saltation-abrasion and total-load models previously (Sklar and Dietrich, 2004; 2006; 2008; Lamb et al., 2008). Models were run by varying one of either grain size, channel slope, or flow depth while holding the remaining two variables constant.

Under constant sediment load, parameterizations of the total-load and saltation-abrasion models generally agree within the bed load regime (τ_*/τ_{*c} < ~20), but diverge within the suspension-regime (Fig. DR3A). The saltation-abrasion model predicts that erosion rates tend towards zero as the threshold for suspension is approached regardless of how changes in transport capacity are achieved (thin gray lines in Fig. DR3A), in contrast to total-load model predictions (black lines in Fig. DR3A). When transport stage varies with grain size (as was the case for the abrasion mill experiments presented here), the total-load model predicts erosion rates decrease with increasing τ_*/τ_{*c} due to reduced kinetic energy of fine grain impacts, asymptotically approaching zero erosion near the threshold for viscous dampening (dashed black line in Fig. DR3). For transport stage varying with flow depth (black dashed-dotted line), or varying with slope (solid black line), both of which are likely in field situations but which we were unable to test experimentally, the total-load model predicts non-zero erosion rates. Increases in transport stage reduce near-bed sediment concentration due to faster particle advection and the lofting of a portion of the sediment load above the bedload layer as particles enter suspension. These effects decrease the number of particle impacts, and in turn, erosion rates. For the case of varying slope, decreases in near-bed sediment concentration are offset by increases in impact velocity for τ_*/τ_{*c} > ~100, such that suspension-regime erosion rates match and can exceed bed load-regime erosion rates (see Lamb et al. (2008) for further discussion).

Bedrock erosion in mountain channels occurs during floods large enough to mobilize bed-sediment, and increases in flood-magnitude generally yield increases in sediment supply (e.g., Leopold et al., 1964). Repeating the above analysis for sediment supply proportional to transport capacity (Fig. DR3B) gives markedly different total-load model predictions than under constant sediment supply (Fig. DR3A), as setting $q_s = 0.5q_{sc}$ maximizes erosion rates for a given grain size and shear velocity (Sklar and Dietrich, 2004). When transport stage is varied by reducing grain size, erosion rates decrease with transport stage well before the threshold for suspension in the saltation-abrasion model is reached (thin gray dashed line in Fig. DR3B), because increased sediment supply does not offset the effect of reduced kinetic energy of impact for fine grains. When transport stage is varied by changing shear velocity, total-load erosion rates increase monotonically with τ_*/τ_{*c} (solid and dashed-dotted black lines in Fig. DR3B), and suspension-regime erosion rates can exceed bedload regime erosion rates by multiple orders of magnitude. Thus, for large-magnitude floods in bedrock rivers, we expect suspension-regime erosion to contribute significantly to, and in cases dominate, the total fluvial abrasion signal, as likely occurred during typhoon-induced storms in the Da'an River, Taiwan (Cook et al, 2012). Additionally, in the suspension regime, bedrock erosion can occur even if the sediment supply exceeds the bedload transport capacity, because the excess sediment, which otherwise would form a static cover and protect the bed, can be transported as suspended load.

Saltation-abrasion and total-load erosion rate predictions can also be compared to those predicted using a stream power model (e.g., Howard and Kerby, 1983),

$$E = K\tau^{\gamma} \qquad \text{(DR3)}$$

where we set K = 0.41 mm / (year Pa) and $\gamma = 1$ to match the observed long-term erosion rates in the South Fork Eel River (Sklar and Dietrich, 2006). Unlike the saltation-abrasion and total-load models, stream power predicts monotonically increasing erosion rate with transport stage, independent of sediment supply, slope, flow depth, or grain size (thick gray dashed line in Fig. DR3). When sediment supply is proportional to sediment transport capacity, the ratio of suspension-regime to bedload-regime erosion rates predicted by the total-load model roughly matches that predicted by stream-power for $2 < \tau_* / \tau_{*c} <$ ~200 (Fig. DR3B).

5. DA'AN RIVER SUSPENSION CALCULATIONS

We calculated u_* / w_s in the Da'an River, Taiwan for all reaches in which Cook et al. (2012) report data (their Table III) for a characteristic typhoon-induced flood discharge of 1300 m^3/s. We solved for shear velocity by combining Equations DR1 and DR2 using reported values of non-dimesnional Shields stress and the medium grain diameter (D = 15 cm) (Cook et al., 2012). We estimated terminal settling velocity for a range of particle sizes using the Dietrich (1982) empirical formula with values appropriate for natural particles (Corey Shape Factor = 0.8; Powers Roundness = 3.5), and defined the maximum grain size expected to be in the suspension regime, D_{susp}, as the largest grain for which $u_*/w_s \geq 1$ (Table DR3). Note that Cook et al. (2012) removed the constraint suppressing suspension-regime erosion in their implementation of the saltation-abrasion model such that they calculated non-zero erosion rates in reaches within the suspension regime. Viscous dampening of particle impacts is not expected to influence abrasion rates for floods which produced measurable erosion in the Da'an River due to the presence of coarse bed-material and large particle Stokes numbers.

DATA REPOSITORY FIGURE AND MOVIE CAPTIONS:

Figure DR1. (A) Mass erosion rate (E_m) and (B) volumetric erosion rate (E_v) for foam, rock, and concrete versus tensile strength (σ_T). Solid lines in (A) and (B) show power-law best fit to the data subject to the theoretical expectation that $E \propto \sigma_T^{-2}$ (Sklar and Dietrich, 2004). The similar scaling between erosion rate and tensile strength for variable-density foam and natural rock suggests that foam is a suitable rock analog. Circled triangles and dots correspond to the foam (σ_T = 0.32 MPa) and limestone (σ_T = 9.8 MPa) used in erosion-rate versus grain-size experiments (Figs. 3 and 4; Table DR1). Mass erosion rates from Sklar and Dietrich (2001) were converted to volumetric erosion rates using densities provided by L. Sklar (personal communication, 2014).

Figure DR2. Side view and bottom-up view photographs showing sediment transport for five different grain sizes in abrasion mill experiments. White arrows indicate flow direction. For both cases, an unerodible clear bed was used for easier visualization. For bottom-up view photographs, note the orientation of particle streaks (due to slow shutter speed) indicate transport dominantly in the azimuthal flow direction. The sediment free area at the center of the mill is the location where the propeller-induced vortex impinges on the bed. In side view photos, ruler on right shows units of cm; in bottom view photographs, the abrasion mill is 20 cm in diameter for scale. Grains of 2.0 and 2.4 mm diameter were intermediate between exclusive bed load and full suspension, moving via long hop lengths, but with hop height rarely exceeding the predicted maximum bedload layer height of ~1.5 cm using the Sklar and Dietrich (2004) empirical relationship.

Figure DR3. Erosion rate predicted with saltation-abrasion, total-load, and stream-power models under variable transport stage ($\tau_*/\ \tau_{*c}$) for conditions representative of the South Fork Eel River, California. Transport stage was varied by changing one of either grain size (D), flow depth (h), or slope (S), while (A) holding sediment supply (q_s) constant or (B) setting sediment supply to half of the transport capacity (q_{sc}). Note the saltation-abrasion model is dependent upon shear velocity, u_* (i.e., the product hS), rather than h or S individually. Following Sklar and Dietrich (2004) we set base values of D, h, S, and q_s to 60 cm, 0.95 m, 0.0053, and 8.9 x 10^{-4} m^2/s, respectively. For all models rock tensile strength was 7 MPa, Young's Modulus was 5 x 10^4 MPa, non-dimensional constant k_v was 10^6, and impacts with particle Stokes numbers < 75 were viscously damped. τ is bed shear stress.

Movie DR1. (MovieDR1.mp4) Side view of suspension-regime transport for D = 1.2 mm sand (u_*/w_s = 1.3) taken with a high speed camera (240 frame per second, total elapsed time is ~3.25 seconds).

Movie DR2. (MovieDR2.mp4)View looking up through clear abrasion mill with D = 1.2 mm sand in suspension-regime transport (u_*/w_s = 1.3) taken with a high speed camera (240 frame per second, total elapsed time is ~3.25 seconds). The abrasion mill is 20 cm in diameter.

Movie DR3. (MovieDR3.mp4)Side view of bedload regime transport for D = 6.8 mm gravel (u_*/w_s = 0.44) taken with a high speed camera (240 frame per second, total elapsed time is ~3.25 seconds).

Movie DR4. (MovieDR4.mp4)View looking up through clear abrasion mill of bedload regime transport for D = 6.8 mm gravel (u_*/w_s = 0.44) taken with a high speed camera (240 frame per second, total elapsed time is ~3.25 seconds). The abrasion mill is 20 cm in diameter. Note radial particle velocity due to secondary circulation exists, but is substantially smaller than azimuthal particle velocity.

DATA REPOSITORY REFERENCES

Beyeler, J.D., Sklar, L.S., Litwin, K., Johnson, J.P., Collins, G.C., and K.X. Whipple, 2009, The dependence of bedrock erodibility on rock material properties: Is tensile strength enough?: American Geophysical Union Fall Meeting, Abstract EP21C-0616, San Francisco, CA.

Cook, K. L., Turowski, J. M., and Hovius, N., 2012, A demonstration of the importance of bedload transport for fluvial bedrock erosion and knickpoint propagation: Earth Surface Processes and Landforms, v. 38, no. 7, p. 683-695, doi:doi: 10.1002/esp.3313.

Dietrich, W. E., 1982, Settling velocity of natural particles: Water Resources Research, v. 18, no. 6, p. 1615-1626, doi:10.1029/WR018i006p01615.

Dietrich, W. E., and Smith, J. D., 1983, Influence of the point-bar on flow through curved channels: Water Resources Research, v. 19, no. 5, p. 1173-1192, doi:10.1029/WR019i005p01173.

Engle, P., 1978, Impact wear of materials: New York, Elsevier Science.

Fernandez-Luque, R., and R. van Beek, 1976, Erosion and transport of bedload sediment: Journal of Hydrualic Research, v. 14, p. 127-144, doi:10.1080/00221687609499677.

Howard, A. D., and Kerby, G., 1983, Channel changes in badlands: Geological Society of America Bulletin, v. 94, no. 6, p. 739-752.

Lamb, M. P., Dietrich, W. E., and Sklar, L. S., 2008, A model for fluvial bedrock incision by impacting suspended and bed load sediment: Journal of Geophysical Research-Earth Surface, v. 113, no. F3, doi:10.1029/2007jf000915.

Leopold, L. B., Wolman, M. G., and Miller, J. P., 1964, Fluvial processes in geomorphology, San Francisco, W.H. Freeman and Company.

McLean, S. R., 1992, On the calculation of suspended-load for noncohesive sediments: Journal of Geophysical Research-Oceans, v. 97, no. C4, p. 5759-5770, doi:10.1029/91jc02933.

Nikora, V., and Roy, A. G., 2012, Secondary flows in rivers: Theoretical framework, recent advances, and current challenges, *in* Church, M., Biron, P. M., and Roy, A. G., eds., Gravel-bed rivers: Processes, tools, environments, John Wiley & Sons, West Sussex, United Kingdom, p. 3-22.

Rouse, H. R., 1937, Modern conceptions of the mechanics of turbulence: Trans. Am. Soc. Civ. Eng., v. 102, no. 1, p. 463-543,

Sklar, L. S., and Dietrich, W. E., 2001, Sediment and rock strength controls on river incision into bedrock: Geology, v. 29, no. 12, p. 1087-1090, doi:10.1130/0091-7613(2001)029<1087:sarsco>2.0.co;2.

Sklar, L. S., and Dietrich, W. E., 2004, A mechanistic model for river incision into bedrock by saltating bed load: Water Resources Research, v. 40, no. 6, doi:10.1029/2003wr002496.

Sklar, L. S., and Dietrich, W. E., 2006, The role of sediment in controlling steady-state bedrock channel slope: Implications of the saltation-abrasion incision model: Geomorphology, v. 82, no. 1-2, p. 58-83, doi:10.1016/j.geomorph.2005.08.019.

Sklar, L. S., and Dietrich, W. E., 2008, Implications of the saltation-abrasion bedrock incision model for steady-state river longitudinal profile relief and concavity: Earth Surface Processes and Landforms, v. 33, no. 7, p. 1129-1151, doi:10.1002/esp.1689.

Winterstein, T., and Stefan, H., 1983, Suspended sediment sampling in flowing water: Laboratory study of the effects of nozzle orientation withdrawal rate and particle size: Saint Anthony Falls Laboratory, External Memorandum M-168, University of Minnesota, 97 p.

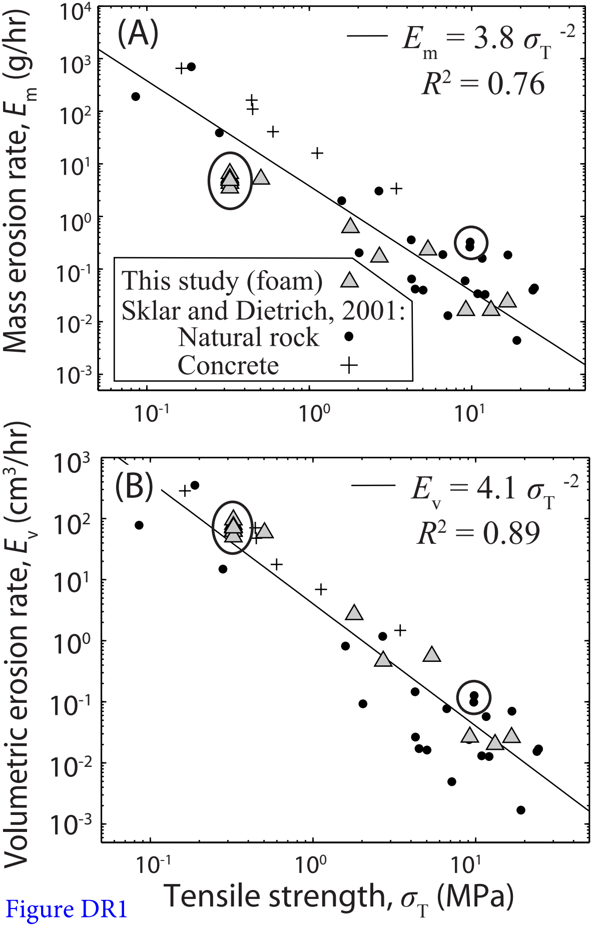

(A)
$E_m = 3.8\ \sigma_T^{-2}$
$R^2 = 0.76$
This study (foam)
Sklar and Dietrich, 2001:
Natural rock
Concrete
Mass erosion rate, E_m (g/hr)
10^{-3}
10^{-2}
10^{-1}
10^{0}
10^{1}
10^{2}
10^{3}
10^{4}
(B)
$E_v = 4.1\ \sigma_T^{-2}$
$R^2 = 0.89$
Volumetric erosion rate, E_v (cm^3/hr)
10^{-3}
10^{-2}
10^{-1}
10^{0}
10^{1}
10^{2}
10^{3}
10^{-1}
10^{0}
10^{1}
Tensile strength, σ_T (MPa)

Figure DR1

Figure DR2

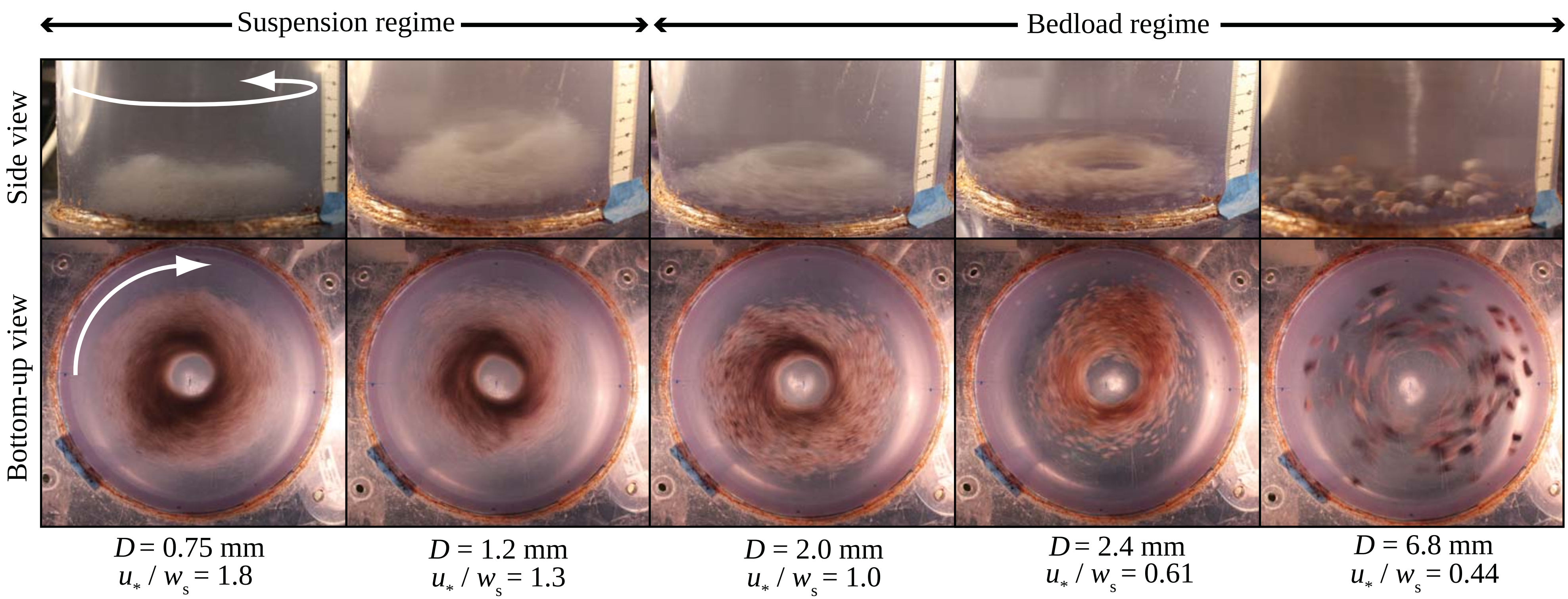

Suspension regime
Bedload regime
Side view
Bottom-up view
D = 0.75 mm
u_* / w_s = 1.8
D = 1.2 mm
u_* / w_s = 1.3
D = 2.0 mm
u_* / w_s = 1.0
D = 2.4 mm
u_* / w_s = 0.61
D = 6.8 mm
u_* / w_s = 0.44

Figure DR3

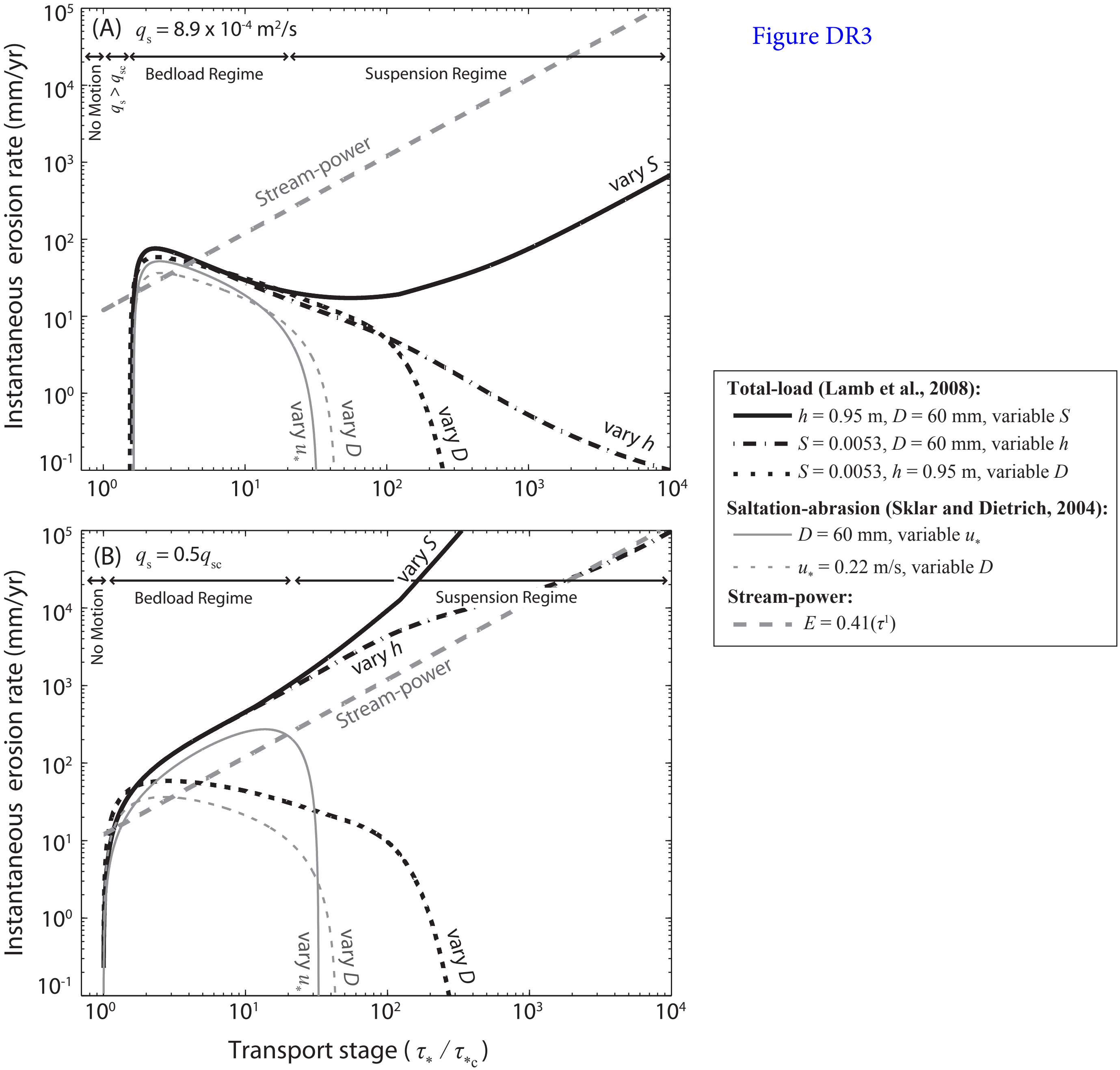

(A) $q_s = 8.9 \times 10^{-4}$ m²/s
No Motion
$q_s > q_{sc}$
Bedload Regime
Suspension Regime
Stream-power
vary S
vary u_*
vary D
vary D
vary h
(B) $q_s = 0.5q_{sc}$
No Motion
Bedload Regime
Suspension Regime
vary S
vary h
Stream-power
vary u_*
vary D
vary D
Instantaneous erosion rate (mm/yr)
Transport stage (τ_* / τ_{*c})
Total-load (Lamb et al., 2008):
h = 0.95 m, D = 60 mm, variable S
S = 0.0053, D = 60 mm, variable h
S = 0.0053, h = 0.95 m, variable D
Saltation-abrasion (Sklar and Dietrich, 2004):
D = 60 mm, variable u_*
u_* = 0.22 m/s, variable D
Stream-power:
$E = 0.41(\tau^1)$

Table DR1: Erosion rates for sediment of varying grain size under constant sediment load and shear stress*

Experiment ID	D_{16} (mm)	D (mm)	D_{84} (mm)	Volume Eroded (cm^3)	Measurement Technique†	Time Eroded (hr)	Volumetric Erosion Rate (cm^3/hr)	u_*/w_s §	% Viscously-Damped Impacts#	Corey Shape Factor	Powers Roundness
D-0.46-A	0.34	0.46	0.58	4.9	Scan	365.4	0.0134	2.9	99.7	0.5	2.5
D-0.46-B	0.34	0.46	0.58	6.1	Scan	365.4	0.0167	2.9	99.7	0.5	2.5
D-0.46-C	0.34	0.46	0.58	4.5	Scan	365.4	0.0122	2.9	99.7	0.5	2.5
D-0.46-D	0.34	0.46	0.58	6.6	Scan	430.0	0.0153	2.9	99.7	0.5	2.5
D-0.46-E	0.34	0.46	0.58	3.2	Scan	430.0	0.00746	2.9	99.7	0.5	2.5
D-0.46-F	0.34	0.46	0.58	4.9	Scan	430.0	0.0113	2.9	99.7	0.5	2.5
D-0.75-A	0.56	0.75	0.99	6.2	Scan	21.0	0.295	1.8	82.3	0.5	2.5
D-0.75-B	0.56	0.75	0.99	5.5	Scan	21.0	0.261	1.8	82.3	0.5	2.5
D-0.75-C	0.56	0.75	0.99	8.7	Scan	21.0	0.413	1.8	82.3	0.5	2.5
D-1.2-A	0.89	1.20	1.58	9.7	Scan	5.0	1.94	1.3	35.5	0.5	2.5
D-1.2-B	0.89	1.20	1.58	12.2	Scan	5.0	2.44	1.3	35.5	0.5	2.5
D-1.2-C	0.89	1.20	1.58	9.9	Scan	5.0	1.97	1.3	35.5	0.5	2.5
D-1.2-D	0.89	1.20	1.58	6.1	Scan	2.5	2.45	1.3	35.5	0.5	2.5
D-2.0-A	1.55	2.02	2.50	25.5	Scan	1.5	17.0	1.00	7.26	0.48	2.5
D-2.0-B	1.55	2.02	2.50	29.8	Scan	1.5	19.8	1.00	7.26	0.48	2.5
D-2.0-C	1.55	2.02	2.50	29.8	Scan	1.5	19.9	1.00	7.26	0.48	2.5
D-2.0-D	1.55	2.02	2.50	23.5	Scan	1.5	15.6	1.00	7.26	0.48	2.5
D-2.4-A	2.0	2.4	2.8	73.0	Scan	1.5	48.6	0.61	3.77	0.69	5
D-2.4-A	2.0	2.4	2.8	60.0	Scan	1.5	40.0	0.61	3.77	0.69	5
D-6.8-A	5.6	6.8	8.0	29.8	Scan	0.3	89.3	0.44	<0.1	0.57	3.5
D-6.8-A	5.6	6.8	8.0	29.8	Scan	0.3	89.3	0.44	<0.1	0.57	3.5
D-6.8-A	5.6	6.8	8.0	58.0	Scan	0.3	174	0.44	<0.1	0.57	3.5
D-24-A	22.0	24.0	26.0	292.2	Scale	1.0	292	0.25	<0.01	0.5	4.5
D-24-B	22.0	24.0	26.0	156.3	Scale	0.5	313	0.25	<0.01	0.5	4.5
D-24-C	22.0	24.0	26.0	73.4	Scale	0.4	176	0.25	<0.01	0.5	4.5
D-24-D	22.0	24.0	26.0	40.6	Scale	0.4	97.5	0.25	<0.01	0.5	4.5
D-24-E	22.0	24.0	26.0	39.1	Scale	0.4	93.8	0.25	<0.01	0.5	4.5
D-40-A	-	40.9	-	182.8	Scale	0.5	366	0.16	<0.01	0.65	5.5
D-40-B	-	43.7	-	121.9	Scale	0.5	244	0.15	<0.01	0.65	5.5

[*] For all experiments, sediment loading was 70 g, propeller was set to 1000 RPM, and the substrate was 0.064 g/cm^3 foam with 0.324 MPa tensile strength and 3.92 MPa Young's modulus. Grains 2.02 mm in diameter and smaller were measured via particle image analysis with a Microtrac DIA, and D_{16}, D, and D_{84} are the 16th percentile, median, and 84th percentile grain size of the sediment used for erosion. Grains 2.4 mm in diameter and larger were hand sieved and manually measured; for these grains, D_{16}, D, and D_{84} represent the lower limit, average, and upper limit of the particle distribution, respectively. A single grain was used where D_{16} and D_{84} are not reported.

[†] Scan refers to eroded volume measured with sub-mm precision laser scanning, and scale refers to mass eroded measured with 0.1-g precision dry-weighing before and after experiments. The two methods gave similar results when both were performed, for certain cases mass loss measurements were advantageous over volume loss measurements, and vice versa (for example, low-density foam with small erooded volumes leads to negligible mass loss such that scan measurements are more accurate).

[§] u_* is the fluid shear velocity. w_s is the terminal settling velocity calculated for particles of size D using measured values of Corey Shape Factor and Powers Roundess and the Dietrich (1982) empirical formula.

[#] Percent of viscously damped impacts was calculated for particles of size D assuming damping of impacts for Stokes numbers <75, and impact velocities based on particle fall height and Gaussian turbulent fluctuations as parametrized in Lamb et al (2008).

Table DR2: Erosion rate for foam of varying tensile strength and Young's modulus*

Experiment ID	Tensile Strength (MPa)	Young's Modulus (MPa)	Density (g/cm^3)	Run Time (hr)	Mass Loss (g)	Volumetric Erosion Rate (cm^3/hr)
Tensile-1-A	0.32	3.92	0.064	1.0	5.6	87.4
Tensile-1-B	0.32	3.92	0.064	1.0	6.6	103
Tensile-1-C	0.32	3.92	0.064	1.0	4.3	67.1
Tensile-1-D	0.32	3.92	0.064	1.0	5.2	81.2
Tensile-1-E	0.32	3.92	0.064	1.0	4.3	67.1
Tensile-1-F	0.32	3.92	0.064	2.0	7.0	54.6
Tensile-1-G	0.32	3.92	0.064	2.0	10.0	78.0
Tensile-1-H	0.32	3.92	0.064	2.0	9.7	75.7
Tensile-1-I	0.32	3.92	0.064	0.7	21.0	447
Tensile-2	0.50	5.38	0.096	4.0	20.6	53.6
Tensile-3	1.79	25.58	0.240	18.0	11.1	2.57
Tensile-4	2.70	47.18	0.320	67.0	11.4	0.531
Tensile-5	5.38	104.80	0.481	71.4	16.6	0.484
Tensile-6	9.20	186.04	0.641	121.2	2.0	0.026
Tensile-7	13.17	265.79	0.769	121.2	2.0	0.021
Tensile-8	16.62	329.56	0.961	168.0	4.0	0.025

* For all experiments, sediment loading was 150 g of 5.6-6.3 mm sieved grains, and propeller was set to 1000 RPM. Mass loss measurements were made by weighing discs before and after the experiment with a 0.1-g precision scale. Eroded discs are commercially available closed cell polyurethane foam (http://precisionboard.com). Tensile strength and Young’s modulus are measured by the manufacturer using standard procedures (American Society for Testing and Materials standard D-1623).

Table DR3: Da'an River suspension calculations[*]

Reach	**Shields Stress**	**Bed Shear Stress (Pa)**	***D*** $_{susp}$ † **(cm)**	**Transport Stage**[§]
Pre-uplift/upstream of uplift	0.091	221	0.98	2.0
Pond in 1999	0.016	38.8	0.19	0.36
Upstream of hinge	0.081	197	0.86	1.8
Downstream of hinge	0.18	437	2.2	4.0
Scarp/knickpoint in 2001	1.02	2480	15	23
Pond in 2004	0.047	114	0.50	1.0
Narrow knickpoint	50.6	123000	110	1100
Knickzone	0.4	971	6.1	8.9
Gorge downstream of knickzone in 2010	0.11	267	1.2	2.4

[*] Shields stress data and reach naming convention as reported by Cook et al. (2012). All calculations based on a water discharge of 1300 m^3/s.

[†] D_{susp} is the largest grain size capable of being within the suspension regime for the reported bed shear stress.

[§] Transport stage calculated assuming a critical Shields Stress of 0.045 (Cook et al., 2012).